Supporting Information for

Efficient Identification of Hydrophobic MOFs: Application in the Capture of Toxic Industrial Chemicals

Peyman Z. Moghadam[1#], David Fairen-Jimenez[2#] and Randall Q. Snurr[1*]

[1]Department of Chemical and Biological Engineering, Northwestern University, Evanston, Illinois, 60208, USA

[2]Department of Chemical Engineering & Biotechnology, University of Cambridge, Pembroke Street, Cambridge CB2 3RA, United Kingdom

# These authors contributed equally to this work

* Corresponding author: snurr@northwestern.edu

Force field parameters for adsorbates

Lennard-Jones (LJ) parameters and partial charges for water were taken from the TIP4P[1] model, and parameters for ammonia and methane were taken from the TraPPE[2,3] model. Table S1 shows the LJ parameters and charges for all of the adsorbates studied in this work.

Table S1. LJ parameters and partial charges for water, ammonia, and methane

Atom	ϵ/k (K)	σ (Å)	Charge (e)	Force field
O_H_2O	78.0	3.15	-	TIP4P[1]
H_ H_2O	-	-	0.52	
M_H_2O	-	-	-1.04	
N_NH_3	185.0	3.42	-	TraPPE[2]
H_ NH_3	-	-	0.41	
M_ NH_3	-	-	-1.23	
CH_4	148.0	3.73	-	TraPPE[3]

Force field parameters for MOFs

LJ parameters for all hypothetical MOFs were taken from the Universal force field (UFF)[4] and partial charges were calculated from the extended charge equilibrium method.[5] The LJ parameters and partial atomic charges for ZIF-8, Al(NDC), and Zn-pyrazole were taken from our previous publication.[6] Force field parameters for MIL-47 were obtained from the work of Yazaydin et al.[7] For FMOF-1, UFF was used for LJ parameters and the partial charges on CF_3 groups were taken from the work of Dalvi et al.[8] Partial charges for C and F atoms in CF_3 group are +0.51 and -0.17, respectively. The partial charges for all other atoms in FMOF-1 were obtained from DFT calculation on a representative FMOF-1 cluster using the B3LYP functional and the 6-31+G* basis set in Gaussian 09[9]. The charges were extracted using the CHELPG method.[10]

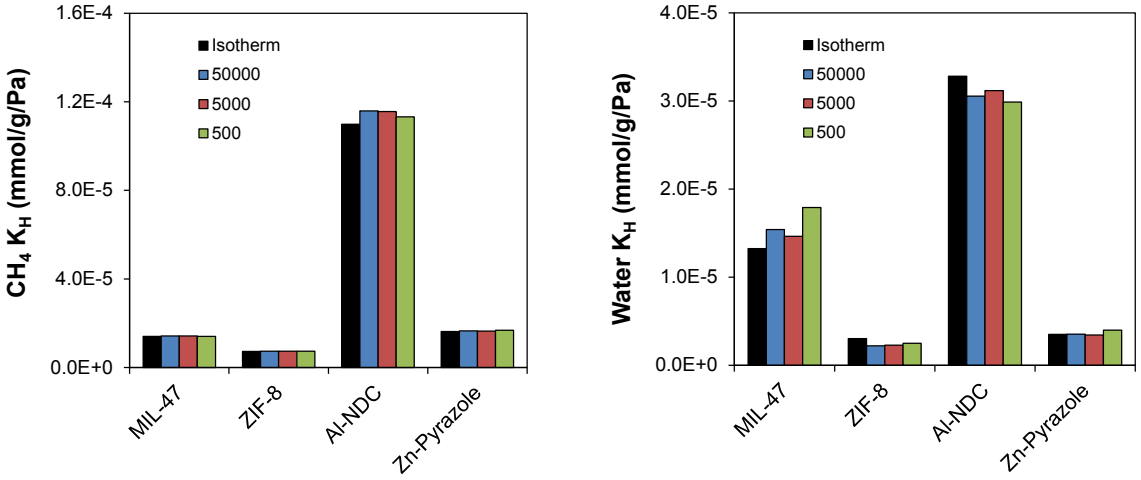

Figure S1. Henry's constant (K_H) values for selected MOFs obtained from either simulated isotherms (GCMC, in black) or from the Widom method with different numbers of cycles (blue, red, green) for methane (left) and water (right) at 298 K. The number of Widom insertions is 20 times the number of cycles.

Simulated water adsorption isotherm in FMOF-1

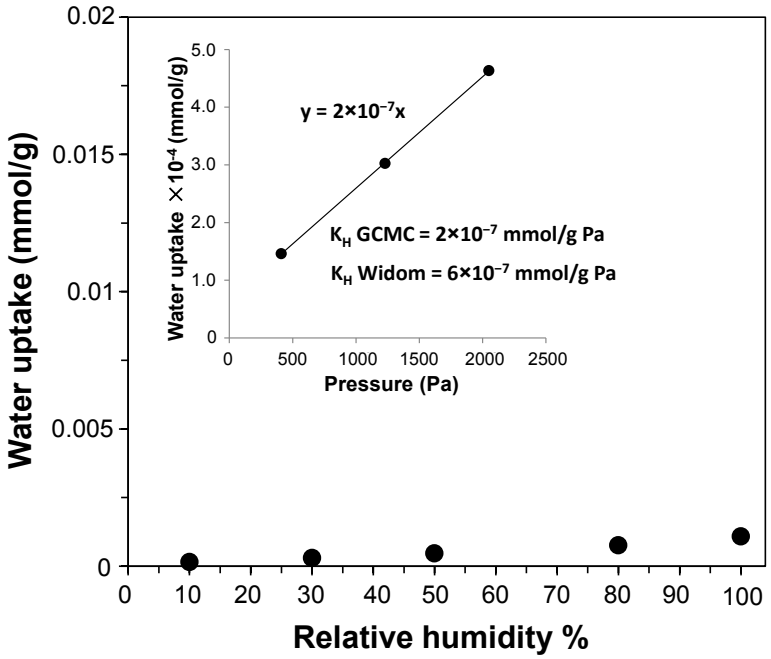

Figure S2. Simulated water adsorption isotherm in FMOF-1 at 298 K. The inset shows the low pressure range and the water K_H values obtained from the isotherm and the Widom insertion method.

Water K_H calculations from experimental adsorption isotherms

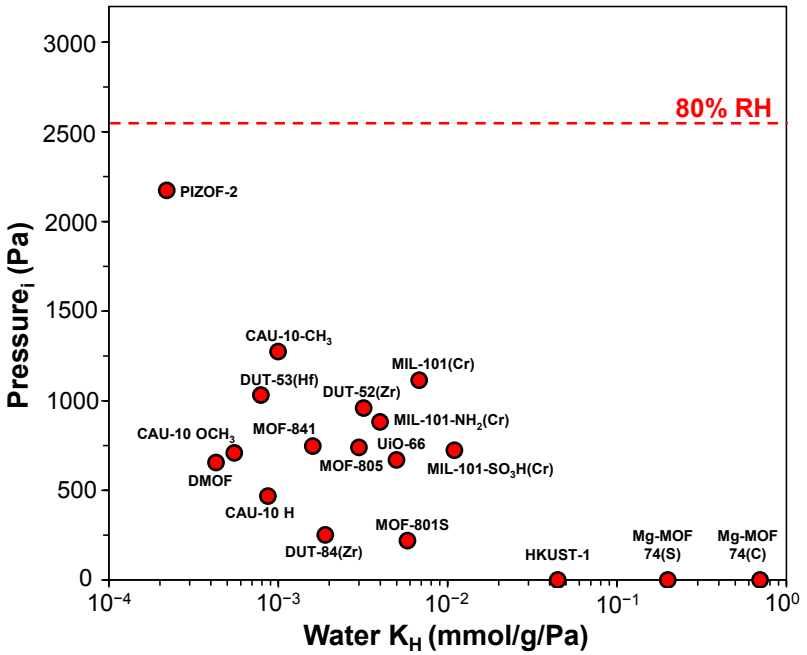

Figure S3. Water condensation pressures versus Henry's constants (K_H) for 19 selected MOFs obtained from experimental water isotherms at room temperature. For Mg-MOF-74, the K_H value has been calculated from two different isotherms. The condensation pressure for the three very hydrophilic MOFs (HKUST-1, Mg-MOF-74(S), and Mg-MOF-74(C)) are set to zero.

PIZOF-2[11]

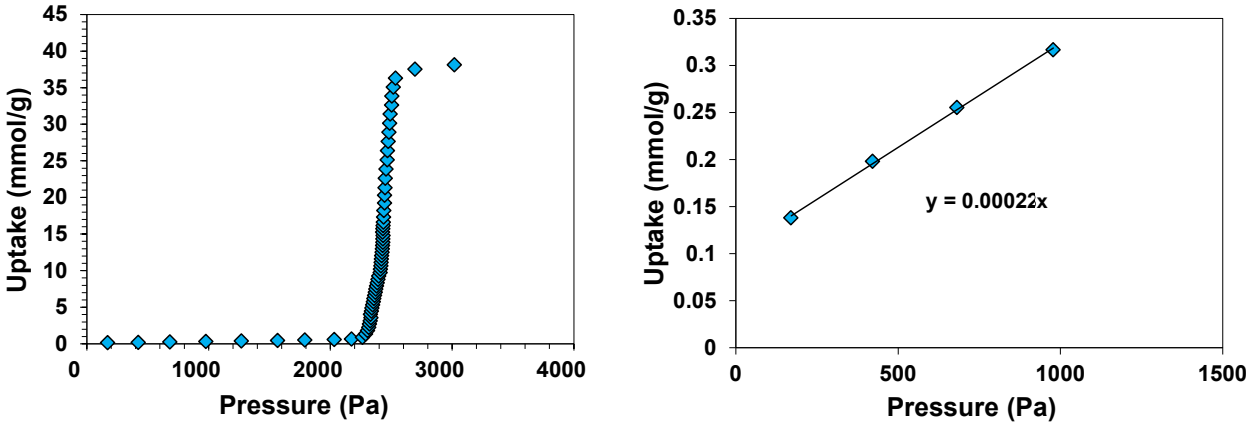

MOF-801(S)[11]

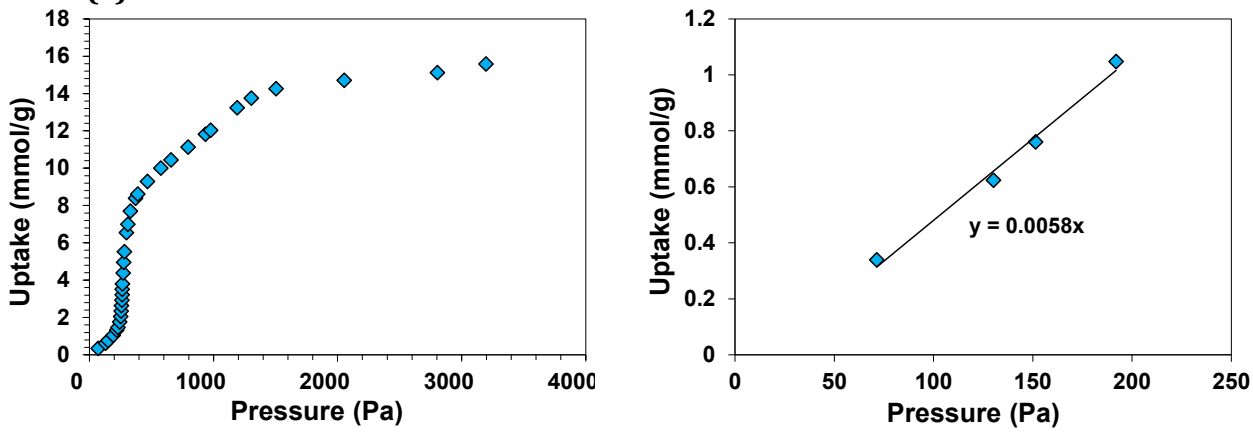

MOF-805[11]

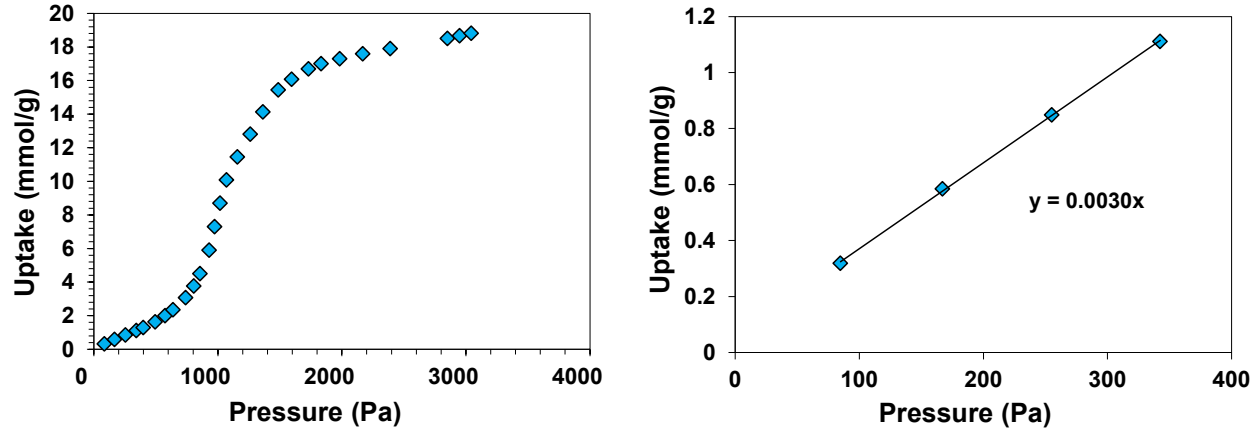

Figure S4. Experimental water adsorption isotherms and the adsorption range selected for Henry's constant (K_H) calculations in MOFs shown in Figure S3.

MOF-841[11]

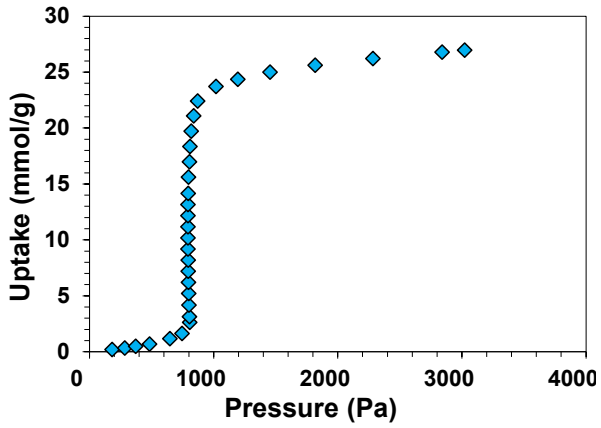

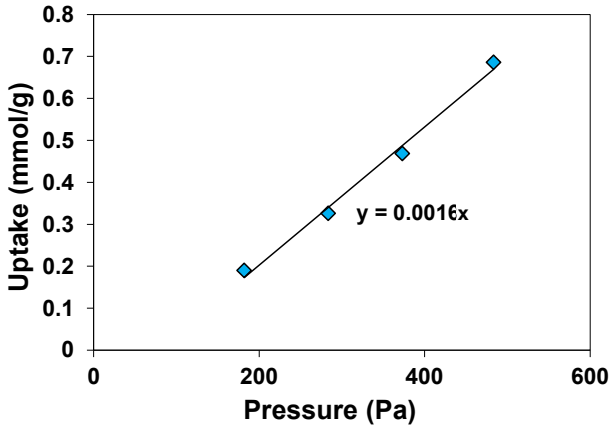

MIL-101(Cr)[12]

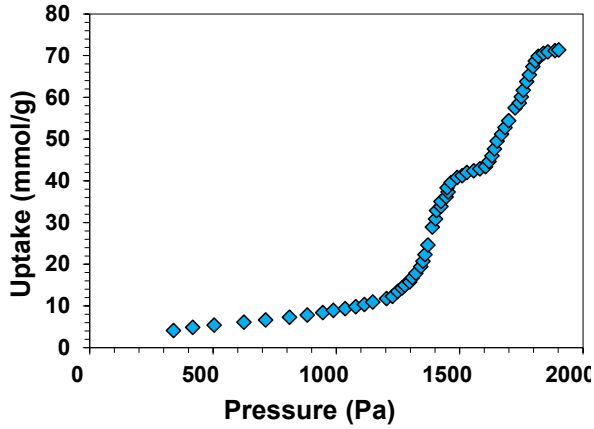

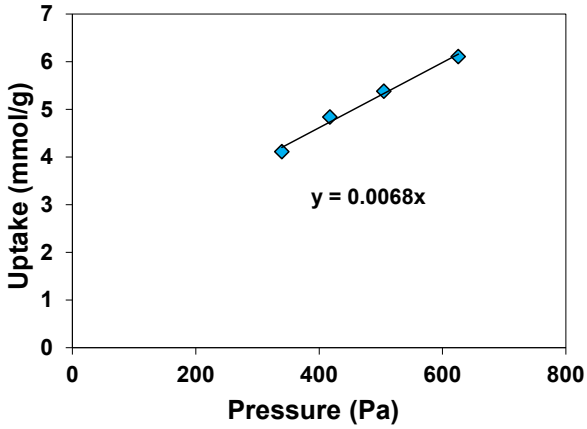

MIL-101-NH_2(Cr)[12]

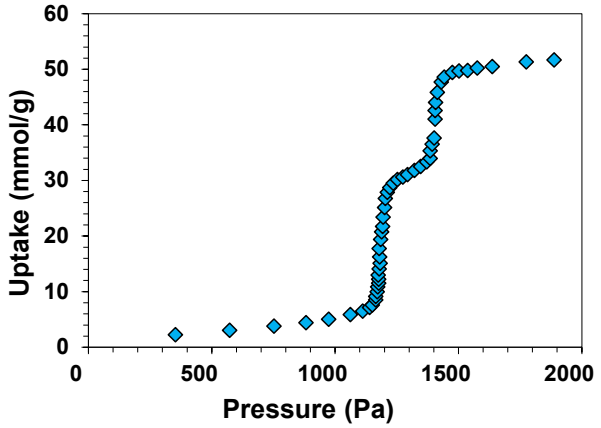

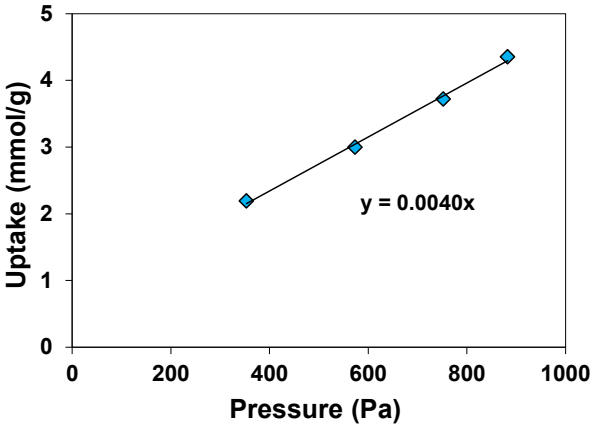

Figure S4. Continued.

MIL-101-SO_3H(Cr)[12]

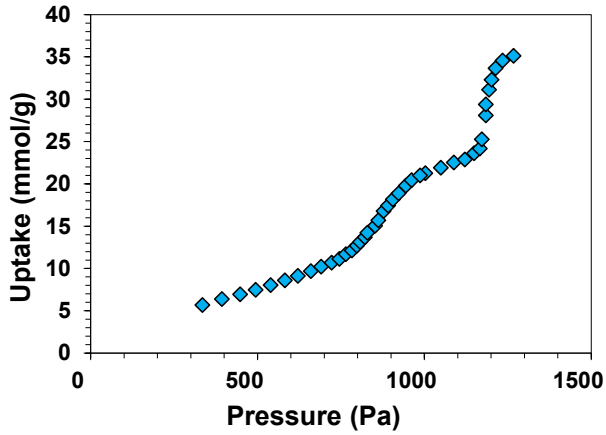

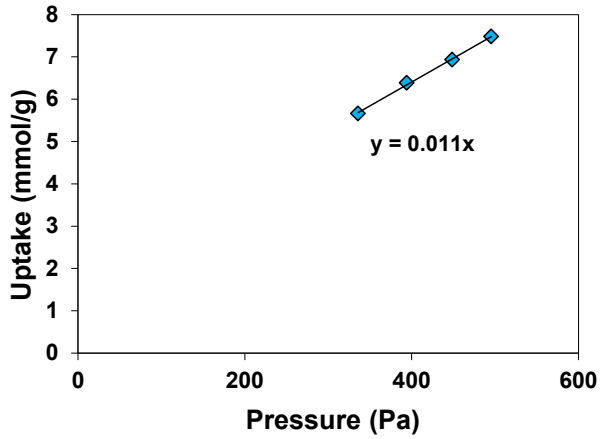

DUT-52(Zr)[13]

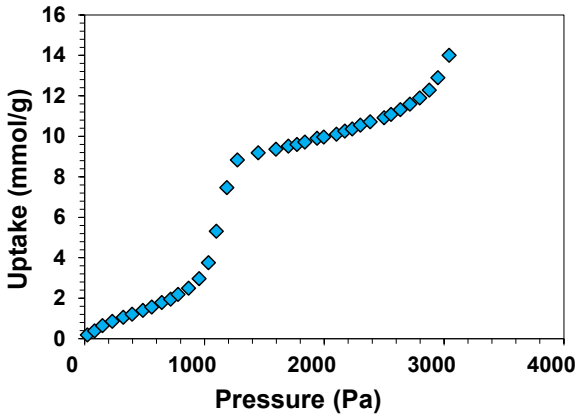

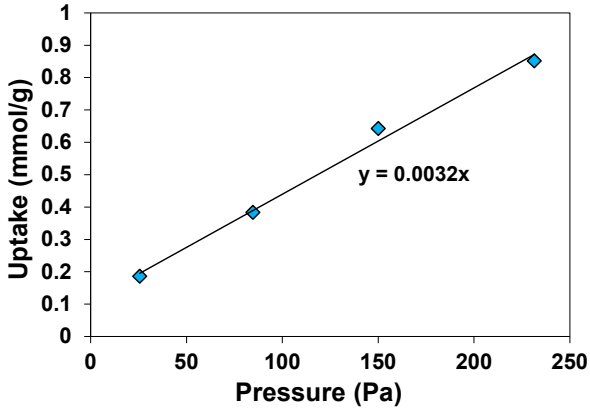

DUT-53(Hf)[13]

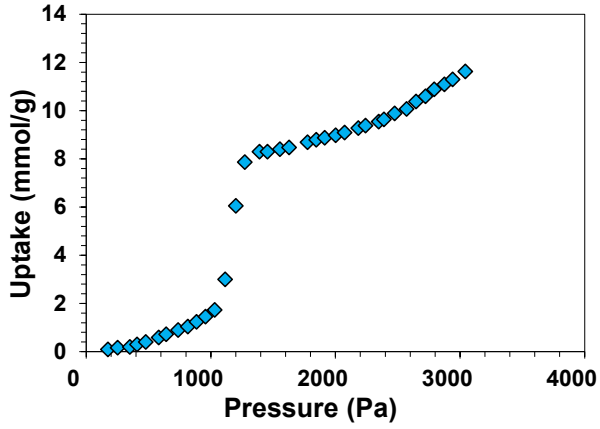

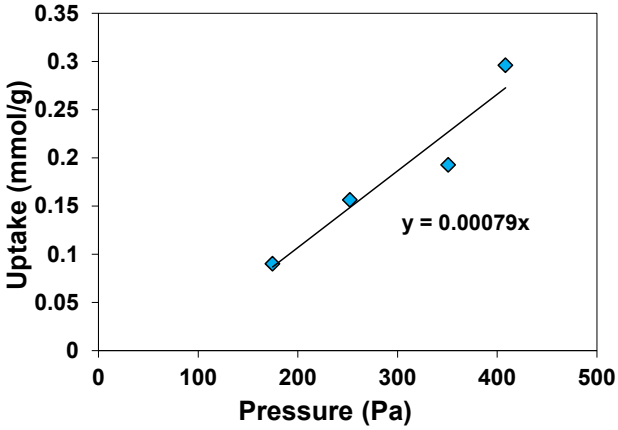

Figure S4. Continued.

DUT-84(Zr)[13]

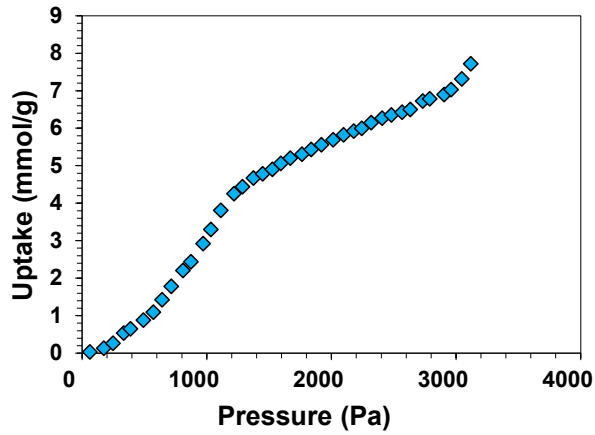

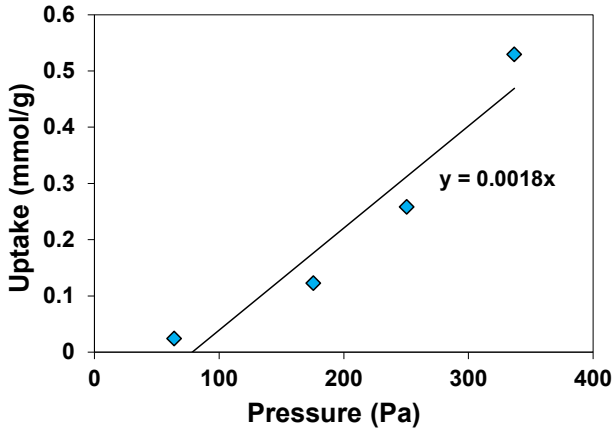

CAU-10 [14]

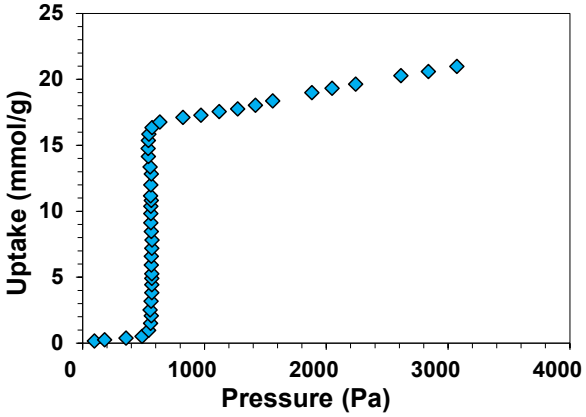

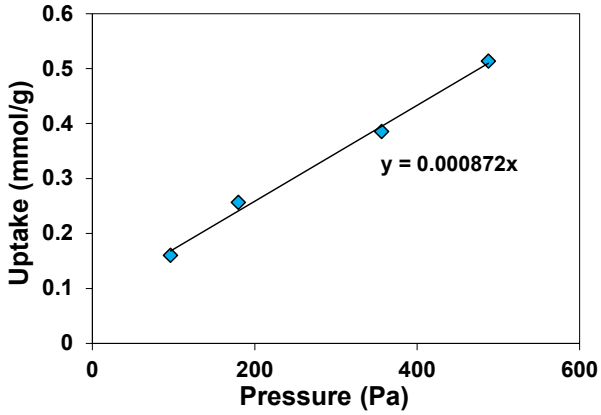

CAU-10-CH_3[14]

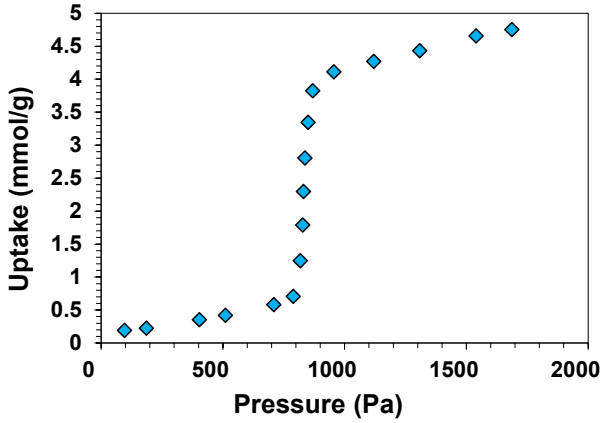

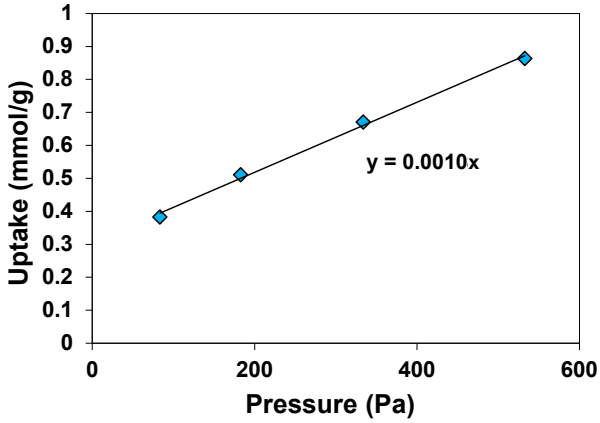

Figure S4. Continued.

CAU-10-OCH$_3$[14]

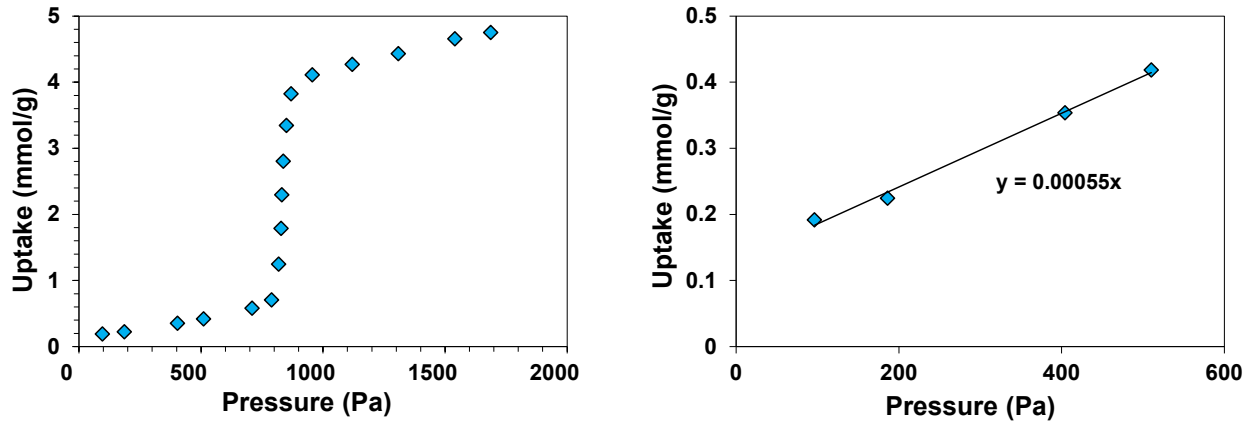

DMOF[15]

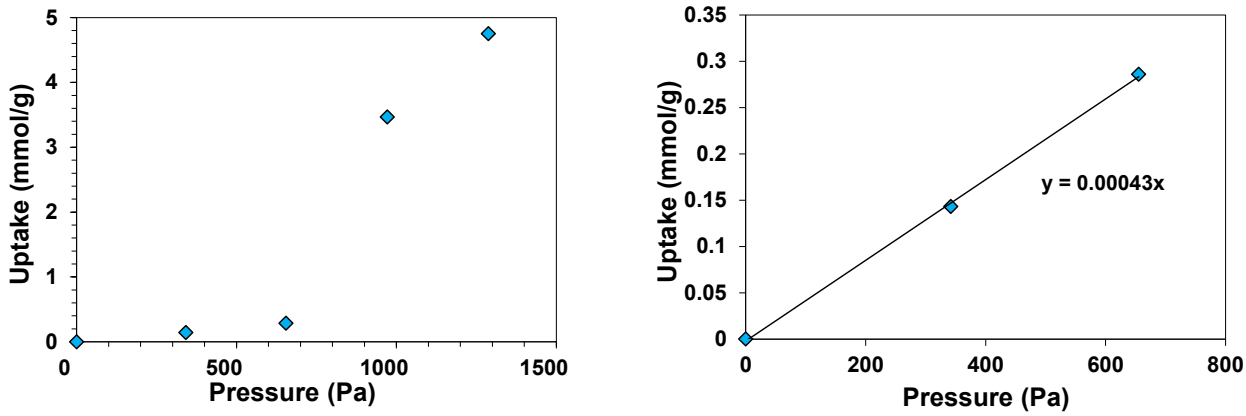

UiO-66[16]

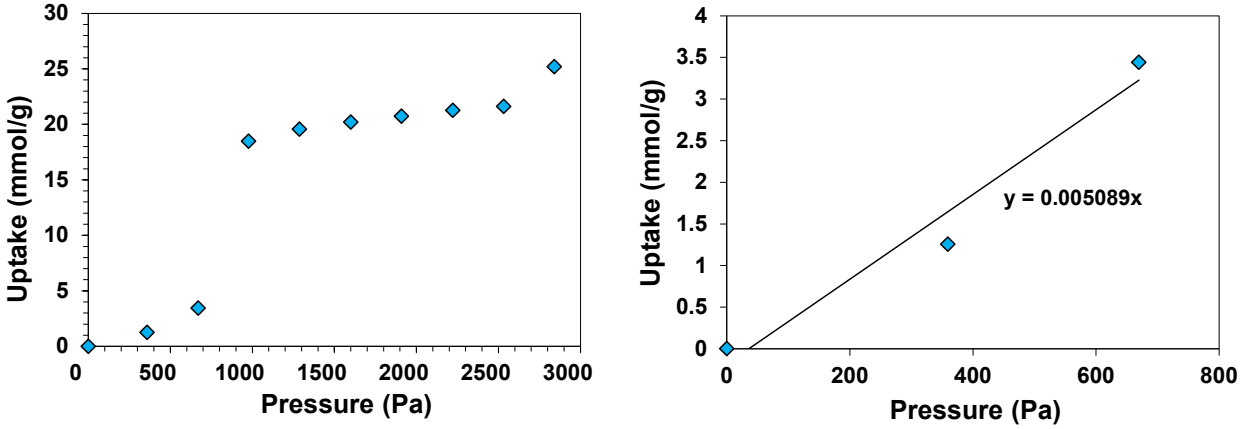

Figure S4. Continued.

Mg-MOF-74(C)[17]

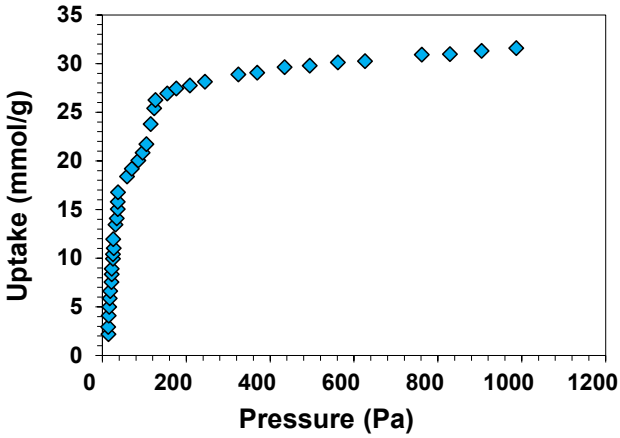

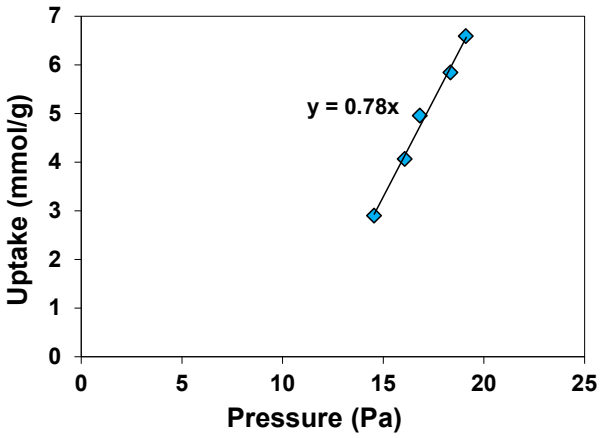

Mg-MOF-74(S)[17]

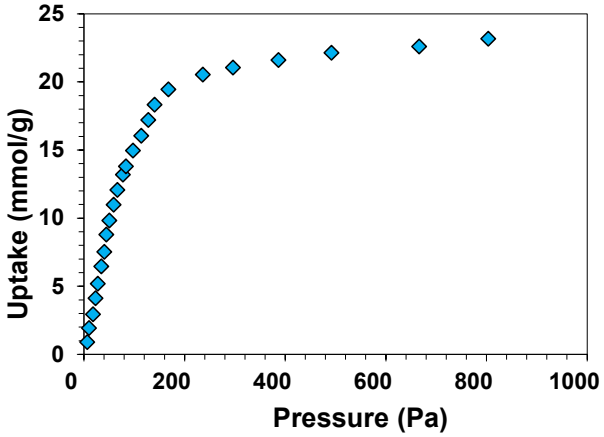

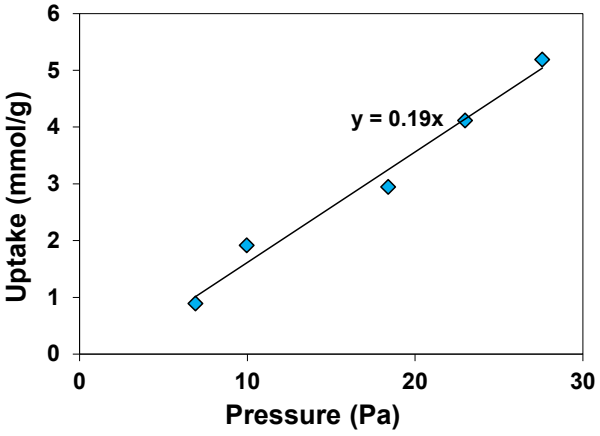

Cu-BTC[16]

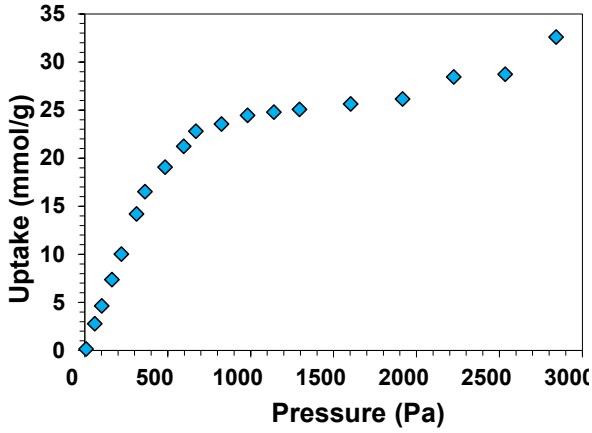

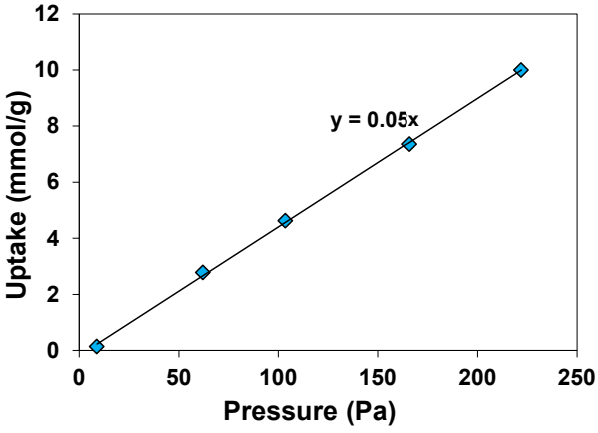

Figure S4. Continued.

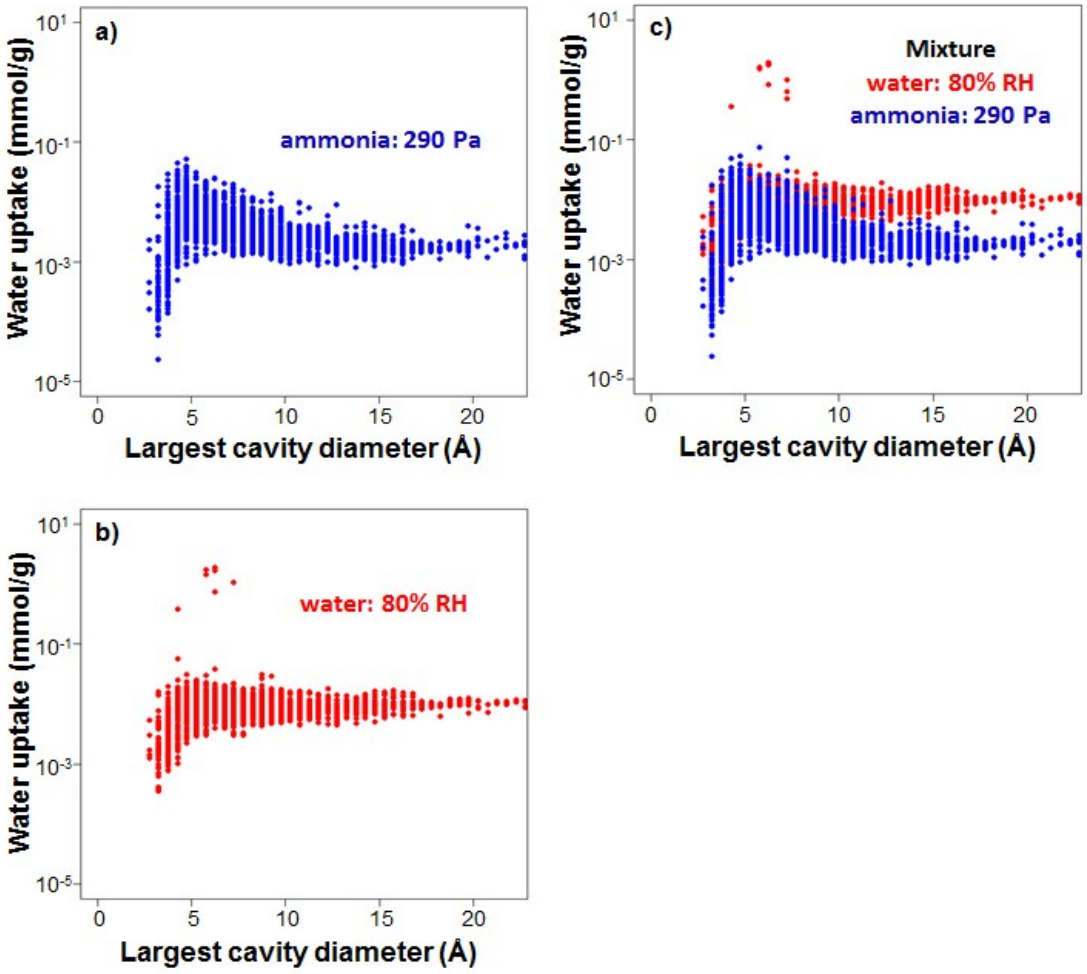

Figure S5. Simulated adsorption amounts for a) pure-compoment ammonia at 290 Pa, b) pure-component water at 80% RH, c) binary mixture of ammonia at 290 Pa and water 80% RH. All simulations were performed for 2,777 unfunctionalized hydrophobic MOFs at 298 K.

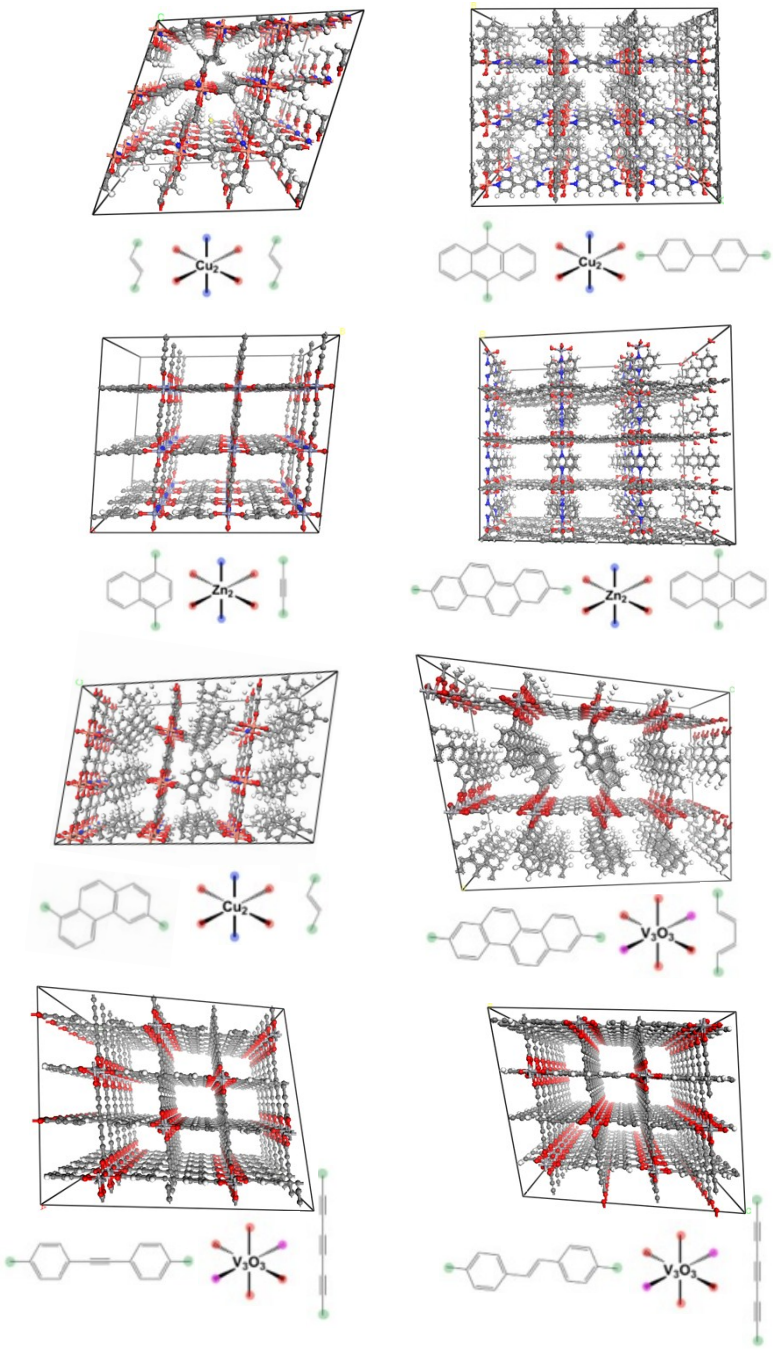

Figure S6. Eight of the 97 hypothetical MOFs with ammonia uptake greater than 6 mmol/g at 100,000 Pa and 298 K. The constituent building blocks for each MOF are shown below the crystal structures. The connection points are highlighted with different colors. Green points: carboxylic acid or a pyridine termination of the organic linker; Red points: carboxylic acid terminations of the organic linker; Blue points: pyridine terminations of the organic linker; and Pink points: inorganic building block connections to other inorganic build blocks.

References

(1) Jorgensen, W. L.; Chandrasekhar, J.; Madura, J. D.; Impey, R. W.; Klein, M. L. *Journal of Chemical Physics* **1983**, *79*, 926.

(2) Zhang, L.; Siepmann, J. I. *Collection of Czechoslovak Chemical Communications* **2010**, *75*, 577.

(3) Martin, M. G.; Siepmann, J. I. *The Journal of Physical Chemistry B* **1998**, *102*, 2569.

(4) Rappe, A. K.; Casewit, C. J.; Colwell, K. S.; Goddard, W. A.; Skiff, W. M. *Journal of the American Chemical Society* **1992**, *114*, 10024.

(5) Wilmer, C. E.; Kim, K. C.; Snurr, R. Q. *The Journal of Physical Chemistry Letters* **2012**, *3*, 2506.

(6) Ghosh, P.; Kim, K. C.; Snurr, R. Q. *The Journal of Physical Chemistry C* **2013**, *118*, 1102.

(7) Yazaydın, A. Ö.; Snurr, R. Q.; Park, T.-H.; Koh, K.; Liu, J.; LeVan, M. D.; Benin, A. I.; Jakubczak, P.; Lanuza, M.; Galloway, D. B.; Low, J. J.; Willis, R. R. *Journal of the American Chemical Society* **2009**, *131*, 18198.

(8) Dalvi, V. H.; Srinivasan, V.; Rossky, P. J. *The Journal of Physical Chemistry C* **2010**, *114*, 15553.

(9) Frisch, M. J.; Trucks, G. W.; Schlegel, H. B.; Scuseria, G. E.; Robb, M. A.; Cheeseman, J. R.; Scalmani, G.; Barone, V.; Mennucci, B.; Petersson, G. A.; Nakatsuji, H.; Caricato, M.; Li, X.; Hratchian, H. P.; Izmaylov, A. F.; Bloino, J.; Zheng, G.; Sonnenberg, J. L.; Hada, M.; Ehara, M.; Toyota, K.; Fukuda, R.; Hasegawa, J.; Ishida, M.; Nakajima, T.; Honda, Y.; Kitao, O.; Nakai, H.; Vreven, T.; Montgomery Jr., J. A.; Peralta, J. E.; Ogliaro, F.; Bearpark, M. J.; Heyd, J.; Brothers, E. N.; Kudin, K. N.; Staroverov, V. N.; Kobayashi, R.; Normand, J.; Raghavachari, K.; Rendell, A. P.; Burant, J. C.; Iyengar, S. S.; Tomasi, J.; Cossi, M.; Rega, N.; Millam, N. J.; Klene, M.; Knox, J. E.; Cross, J. B.; Bakken, V.; Adamo, C.; Jaramillo, J.; Gomperts, R.; Stratmann, R. E.; Yazyev, O.; Austin, A. J.; Cammi, R.; Pomelli, C.; Ochterski, J. W.; Martin, R. L.; Morokuma, K.; Zakrzewski, V. G.; Voth, G. A.; Salvador, P.; Dannenberg, J. J.; Dapprich, S.; Daniels, A. D.; Farkas, Ö.; Foresman, J. B.; Ortiz, J. V.; Cioslowski, J.; Fox, D. J.; Gaussian, Inc.: Wallingford, CT, USA, 2009.

(10) Breneman, C. M.; Wiberg, K. B. *Journal of Computational Chemistry* **1990**, *11*, 361.

(11) Furukawa, H.; Gándara, F.; Zhang, Y.-B.; Jiang, J.; Queen, W. L.; Hudson, M. R.; Yaghi, O. M. *Journal of the American Chemical Society* **2014**, *136*, 4369.

(12) Akiyama, G.; Matsuda, R.; Sato, H.; Hori, A.; Takata, M.; Kitagawa, S. *Microporous and Mesoporous Materials* **2012**, *157*, 89.

(13) Bon, V.; Senkovska, I.; Weiss, M. S.; Kaskel, S. *CrystEngComm* **2013**, *15*, 9572.

(14) Reinsch, H.; van der Veen, M. A.; Gil, B.; Marszalek, B.; Verbiest, T.; de Vos, D.; Stock, N. *Chemistry of Materials* **2013**, *25*, 17.

(15) Jasuja, H.; Burtch, N. C.; Huang, Y.-g.; Cai, Y.; Walton, K. S. *Langmuir* **2013**, *29*, 633.

(16) Schoenecker, P. M.; Carson, C. G.; Jasuja, H.; Flemming, C. J. J.; Walton, K. S. *Industrial & Engineering Chemistry Research* **2012**, *51*, 6513.

(17) Yang, D.-A.; Cho, H.-Y.; Kim, J.; Yang, S.-T.; Ahn, W.-S. *Energy & Environmental Science* **2012**, *5*, 6465.